Divanillin-Based Polyazomethines: Toward Biobased and Metal-Free π-Conjugated Polymers

Guillaume Garbay, Lauriane Giraud, Sai Manoj Gali, Georges Hadziioannou, Etienne Grau, Stéphane Grelier, Eric Cloutet, Henri Cramail, Cyril Brochon

Divanillin based polyazomethines: toward bio-based and metal-free π-conjugated polymers

Guillaume Garbay, [†#a] Lauriane Giraud,[#a] Sai Manoj Gali, [a] Georges Hadziioannou, [a] Etienne Grau,[a] Stéphane Grelier,[a] Eric Cloutet, [a] * Henri Cramail, [a] * Cyril Brochon [a] *

[a] Laboratoire de Chimie des Polymères Organiques (LCPO UMR 5629), CNRS-Université de Bordeaux-Bordeaux INP, 16 Avenue Pey-Berland, Pessac, 33607 Cedex, France

Polyazomethines, Divanillin, Carbazole

ABSTRACT: Divanillin was synthesized in high yield and purity using Laccase from *Trametes versicolor*. It was then polymerized with Benzene-1,4-diamine and 2,7-diaminocarbazole to form polyazomethines. Polymerizations were performed under micro-wave irradiation and without transition-metal based catalyst. These bio-based conjugated polyazomethines present a broad fluorescence spectrum ranging from 400 to 600 nm. Depending on the co-monomer used, polyazomethines with molar masses around 10 kg.mol^{-1} and with electronic gaps ranging from 2.66 to 2.85 eV were obtained. Furthermore, TD-DFT calculations were performed to corroborate experimental results.

1. Introduction.

Thanks to recent works on the selective oxidative coupling of phenolic molecules *via* enzymatic catalysis, a bio-based platform of lignin-derived aromatics is now available.[1,2] Among them, vanillin has a large potential as it is one of the only phenolic compounds industrially available from biorefinery.[3] Vanillin can be easily dimerized from C-C coupling using an environmental-friendly process as was demonstrated by Llevot *et al*..[4] Such divanillin was used as a bio-based aromatic building block for the design of semi-aromatic polymers exhibiting different thermo-mechanical properties.[5] However, divanillin monomer has also the potential to be valorized in the field of organic electronics.[6] Indeed, in addition to the two phenolic functions, such derivative possesses two aldehyde moieties that can be involved in condensation reactions, for instance with amino groups, leading to polyazomethines. Polyazomethines exhibit many advantages as they can be obtained through metal-free polycondensation with water as the only by-product. [7–12] Moreover, polyazomethines can be synthesized under micro-wave irradiation which brings the benefit of being faster and more efficient than conventional heating.[13,14] π-conjugated polyazomethines present a good thermal resistance and are air-stable.[15,16] They possess PPV-like electronic properties, can be tuned to exhibit a high absolute fluorescence quantum yield when doped and exhibit a good chemical and electrochemical resistance.[9,15–22] Interestingly, such polymers could be prepared by selecting diamino-functionalized monomers versus bis-aldehyde divanillin.

In this work, we describe the synthesis of a divanillin monomer substituted by alkyl chains and its subsequent polycendensation with 1, 4-benzene diamine or 2,7-carbazole diamine. The optical and electrochemical properties of the so-formed polyazomethines were also investigated.

2. Results and discussion.

The 6,6-Dihydroxy-5,5-dimethoxy-[1,1-biphenyl]-3,3-dicarboxaldehyde (Divanillin or **DV**) was synthesized from vanillin at room temperature using the procedure already described by us (**Scheme 1**). [1] In ^{1}H NMR, (**Figure SI1**); the signal at 9.7 ppm corresponds to the two aldehyde protons and the signal at 7.5 and 7.2 ppm to the aromatic ones. The signal at 3.8 ppm corresponds to the methoxy groups. The structure of **DV** was also attested by ATR-FTIR (**Figure SI2**).

In order to improve the solubility of **DV** and polyazomethines thereof in classical organic solvents, the latter was alkylated. [9,23,24] Etherification reaction was performed in DMSO in the presence of KOH and 2-ethylhexyl bromide to give Divanillin Ethyl Hexylated or **DVEH** (**Scheme 1**). The alkylation reaction was assessed by ^{1}H NMR spectroscopy and ATR-FTIR (**Figure SI3** and **SI4**); NMR signals around 3.81 ppm and the signals between 0.69 and 1.39 ppm confirmed the completion of alkylation reaction.

The divanillin-based monomer (**DVEH**) was polymerized at the stoichiometry ratio 1:1 both with commercially available benzene-1,4-diamine and 2,7-diaminocarbazole to give respectively **P1** and **P2** (synthesized according to the literature)[12] (**Scheme 1**). The polymerization reaction being performed under micro-wave irradiation which is usually faster than conventional heating.[25,26] Silica was added to the reaction medium to remove water and displace the equilibrium towards the polymer formation. **P1A** and **P2** were obtained after 4 hours of reaction and purified by precipitation in methanol. Interestingly, the use of silica allowed a simple recovery process of the polyazomethine through filtration before precipitation. However, silica is not necessary to carry out the polymerization reaction. Indeed, the synthesis of the polyazomethine was also performed without silica, in just 5 minutes instead of 4h (**P1B**). The crude polyazomethine was then dissolved in methylene chloride; methanol was added and then the solvent was evaporated using a rotary evaporator. The powder obtained was rinsed with methanol, giving the final product **P1C**.

The polyazomethines were characterized by NMR and SEC. ^{1}H NMR signal at 8.5 ppm clearly attested the formation of azomethine bond (-CH=N-) (**Figure SI5 and SI6**). All the molecular characteristics, thermal and optical properties of **DVEH**-based polyazomethines are reported in **Table 1**.

Scheme 1. Alkylation of divanillin with ethylhexyl side chains (DVEH) and polymerization with p-phenylenediamine (P1) and diamino carbazole (P2).

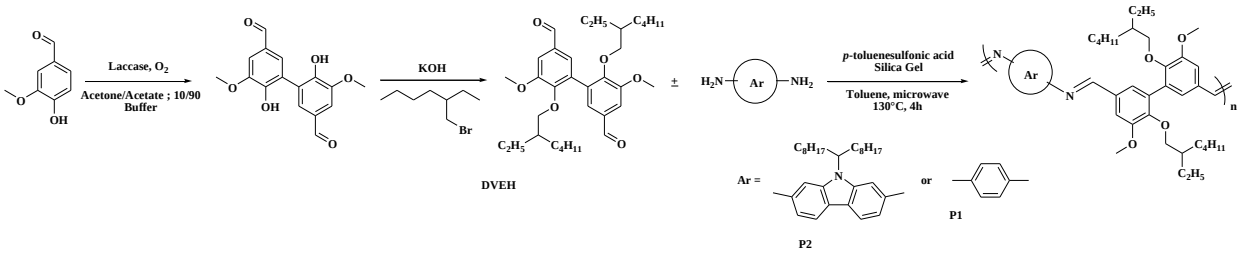

SEC traces show discrete peaks at low molar masses, according to a polycondensation pathway with heavy monomers (**Figure SI7** and **SI8**). Both polymers have a dispersity close to two, which is consistent with a step-growth mechanism (at high conversion). The two families of polyazomethines present apparent number-average molar masses $\overline{M}_n$ of 10600 g.mol^{-1} and 6200 g.mol^{-1} respectively for **P1A** and **P2**, for a reaction time of four hours. For the polyazomethines **P1**, similar molar mass was obtained in just 5 minutes of reaction, after purification. Interestingly, post-condensation was probably occurring during the purification, resulting in a higher molar mass (10000 g/ mol with 70% yield) compared to the crude. It confirms that post-condensation occurs during solvent evaporation.

Thermal properties of the polyazomethines were determined by thermogravimetric analysis under N_2 atmosphere at a heating rate of 10°C per minute. All polyazomethines present a good thermal stability with a degradation temperature around 405°C (**Figure SI9** and **SI10**). The diamine used does not have a significant impact on the thermal stability. In addition, differential scanning calorimetry (DSC) analyses carried out between -80°C and 200°C did not show any specific transition neither glass transition nor crystallinity behavior, indicating the very rigid structure of these polyazomethines and their probable amorphous state (see **Figure SI11** and **SI12**).

All the polyazomethines were characterized by UV-vis absorption and fluorescence spectroscopy analyses. As shown in **Fig. 1**, the carbazole-based polyazomethine main absorption band is red-shifted as compared to the phenyl-based derivative, from 364 to 390 nm. This behavior could be due to a stronger electron-rich/electron-poor couple in the case of the carbazolylene derivative or to a more planar conformation increasing the conjugation length. It is even amplified in fluorescence spectra where the shift can reach 150 nm. This is coherent with the higher molar attenuation coefficient of carbazole compared to the one of the bisvanillin.[27] Both **P1** and **P2** have a weak emission, with a fluorescence quantum yield below 2% in solution.

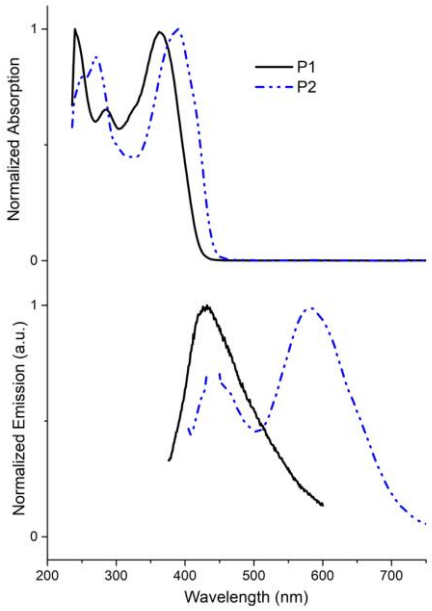

Figure 1. Absorption spectra (top) and emission spectra (excited at 360 nm, bottom) of the two **DVEH**-based polyazomethines **P1A** and **P2** in methylene chloride

Electrochemical features of these polyazomethines were determined by cyclic voltammetry using dichloromethane solutions of tetrabutylammonium hexafluorophosphate ($TBAPF_6$) as electrolyte, silver as reference electrode and platinum for the working and counter-electrodes. Finally, the material was solubilized in the electrolyte solution at a concentration of 0.1 $g.L^{-1}$ (**Figures SI13** and **SI14**). The values of the energy levels are indicated in **Table 2**.

The slight differences between the electrochemical and optical band-gaps can be explained by the fact that the redox peaks result from localized sites rather than from the conjugated backbone.[28] For the 1, 4-diaminobenzene-based polyazomethines, both optical and electrochemical gap are comparable within experimental errors, with a value around 2.67 eV for the electrochemical gap and 2.96 eV for the optical one.

Table 1. **Molar masses, thermal and optical properties of divanillin-based polyazomethines.**

Polyazomethines	Co-monomer of DVEH	Experimental conditions[a]	$\overline{M}_n$ [b] [g.mol^{-1}]	$\overline{M}_w$ [b] [g.mol^{-1}]	$Đ$[b]	$\overline{DP}_n$[b]	T_d[c] [°C]	Absorption [d,e] λ_{sol}^{max} (λ_{film}^{max}) [nm]	Emission [d,e] λ_{sol}^{max} (λ_{sol}^{max}) [nm]
P1A	NH_2-Ph-NH_2	4h, silica, purified	10600	21900	2.1	18	395	285-365 (290-370)	430 (460)
P1B	NH_2-Ph-NH_2	5min, no silica, crude	5700	11500	2	9		285-365 (290-370)	
P1C	NH_2-Ph-NH_2	5min, no silica, purified	10000	20000	2	17			
P2	NH_2-Cbz-NH_2	4h, silica, purified	6200	15400	2.5	7	401	270-390 (ND)	580 (ND)

[a] Under micro-wave irradiation at 130°C, in toluene with APTS as a catalyst [b]Determined by Size Exclusion Chromatography (SEC) relative to polystyrene standards in THF at 40°C. [c]Decomposition temperature at 20% weight loss, evaluated under N_2 at a heating rate of 10 °C/min. [d] Determined in dichloromethane solution, [e] Determined on films obtained by drop-casting on quartz.

Table 2. **Physical properties of divanillin based polyazomethines.**

Polyazomethine	HOMO [eV][a]	LUMO [eV][a]	Eg^{elec} [eV][b]	Eg^{opt} [eV][c]	HOMO[d]	LUMO[d]	E_G[d]
P1A	- 5.21	- 2.36	2.85	3.02	-5.500	-1.911	3.58
P2	- 5.18	-2.50	2.68	2.85	-5.203	-1.808	3.39

[a] Estimated from the oxidation and reduction potentials measured by cyclic voltammetry in CH_2Cl_2 solution. [b] Calculated by difference between oxidation and reduction potentials. [c] Calculated by Tauc method. [d] Calculated by B3LYP/6-31 (d,p) level of theory

In the case of carbazole-based polyazomethine, these values reach respectively 2.66 eV and 2.85 eV. These gap reductions are coherent with the red-shift observed in both absorption and emission spectra.

DFT calculations were carried out on **DV-Ph** and **DV-Cbz** derivatives at B3LYP/6-31 (d,p) level of theory with chloroform as implicit solvent (CPCM). Different angles in both molecules were first estimated (**Figures SI15** and **SI16** and **Table SI1**). The choice of DFT functional employed is based on the closeness of calculated electronic bandgap ($E_G = E_{HOMO} \sim E_{LUMO}$) of monomers (as a function of different DFT functional employed, see **Table SI2** for more details) with respect to experimental values determined by cyclic voltammetry (**Table SI3**). **DV-Cbz** derivative shows lower E_G compared to **DV-Ph** derivative as reported in **Table 2**.

Furthermore, Khun's model was employed to compute the electronic band gap at polymer limit (Equation 1).[29,30]

$$E_g = E_0 \sqrt{1 + D_k \cos\left(\frac{\pi}{N+1}\right)} \quad (1)$$

When $n \to \infty$, n is the number of monomer units in the oligomer, E_o corresponds to electronic transition energy when N = 1, N being number of double bonds along the shortest conjugated pathway between terminal carbon atoms for oligomers of size n (**Figure SI17**). D_k is the force constant that represent the strength of coupling between single and double bonds, implicitly linked to the efficiency of connection between the units in an oligomer. By plotting E_G as a function of number of double bonds (N), it exhibits higher π-conjugation of **DV-Cbz** derivative suggesting a better delocalization of π electrons[31] with respect to

DV-Ph derivatives with values of D_k as 0.818 and 0.748 respectively. (**Table SI4**). These results are in agreement with experimental data.

3. Conclusion.

The synthesis of different polyazomethines embedding divanillin bio-based platform was performed. Divanillin was synthesized and alkylated, then polymerized with two different diamines: 1, 4-benzene diamine and an alkylated 2,7-diaminocarbazole. The polymerization was performed under micro-wave irradiation, without any metallic catalyst and with water as the only by-product. Remarkably, all polyazomethines present a broad emission at the beginning of the visible range. The carbazole-based polyazomethine is red- shifted compared to the phenyl-based one, in the case of both absorption and emission. This bathochromic shift is expected as the carbazole moiety is more electron-donating than the phenyl one. Interestingly, the methodology followed meets some challenges for a "green chemistry" such as lowering the number of steps, avoiding transition metal catalyst and use of bio-based monomers to quote a few. In addition, these new polyazomethines have promising properties (confirmed by TD-DFT calculations) for opto-electronic applications like OLED for example.

These encouraging results pave the way for a whole family of bio-based π-conjugated polyazomethines. Optical properties can be enhanced by optimizing the structure and/or by playing on doping. The extension to other π-conjugated moieties is currently investigated. Furthermore, for a better understanding of optical and electrical properties, small model trimers and dimers will be isolated and fully characterized. All these new development will be discussed in forthcoming papers.

4. Experimental Section

Materials.

Vanillin (>97%), Laccase from Trametes Versicolor, and 2-ethyl hexyl bromide (95%) were obtained from Sigma-Aldrich. Para-toluene sulfonic acid (PTSA, 99%) was purchased from TCI. Silica gel (pore size 60 Å, 230-400 mesh particle size, particle size 40-63 µm) was obtained from Honeywell Fluka. All products and solvents (reagent grade) were used as received except otherwise mentioned. The solvents were of reagent grade quality and were purified wherever necessary according to the methods reported in the literature. Flash chromatography was performed on a Grace Reveleris apparatus, employing silica cartridges from Grace. Cyclohexane: ethyl acetate gradients were used as eluents. The detection was performed through ELSD and UV detectors at 254 nm and 280 nm. The reactions under micro-wave irradiation were performed on a Discover-SP from CEM, with the temperature measured by infrared; the power of the apparatus is constantly adjusted to reach and then stay at the set temperature.

Characterization techniques.

1H, 13C and 1H-13C HSQC NMR measurements were performed with a Bruker Avance 400 spectrometer (400.20 MHz and 100.63 MHz for 1H and 13C, respectively) at room temperature using deuterated solvent.

IR spectra were recorded with Bruker Tensor 27 spectrometer using a 0.6 mm-diameter beam. Samples were analyzed with the attenuated total reflexion (ATR) method.

High resolution mass spectroscopy analyses were performed on an AutoSpec-Waters spectrometer (EI).

Optical absorption spectra were obtained with a UV-visible spectrophotometer (UV-3600, Shimadzu). Photoluminescence spectra were obtained from a spectrofluorometer (Fluoromax-4, Horiba Scientific).

Molar masses of polymers P1A, P1B and P1C measured in THF were determined by size exclusion chromatography (SEC) using a three-columns set of Resipore Agilent: one guard column Resipore Agilent PL1113-1300, then two column Resipore Agilent PL1113-6300, connected in series, and calibrated with narrow polystyrene standards from polymer Laboratories using both refractometric (GPS 2155) and UV detectors (Viscotek). THF was used as eluent (0.8 mL/min) and trichlorobenzene as a flow marker (0.15%) at 30°C.

Molar masses of polymer P2 measured in THF were determined by size exclusion chromatography (SEC) using a three-columns set of TSK gel TOSOH (G2000, G3000, G4000 with pore sizes of 20, 75, and 200Å respectively, connected in series) calibrated with narrow polystyrene standards from polymer Laboratories using both refractometric and UV detectors (Varian). THF was used as eluent (1 mL/min) and trichlorobenzene as a flow marker at 40°C.

Molar masses of polymer samples in $CHCl_3$, were measured by SEC at 40°C with THF as eluent, using a Viscotek VE2001-GPC. Polymer laboratories-Varian (one guard column and three columns based on cross-linked polystyrene, pore size = 200 Å, 75 Å and 20 Å), and PS standards were used for calibration.

TGA have been performed on a TA-Q50, from 25°C to 600 - 700 °C with a heating of 10°C.min-1 under nitrogen flow.

DSC analysis have been performed on a TA instrument, under Helium flow, with an LN_2 cooling and modulated with +/- 0.64 °C every 60 seconds. Sample were heated at 10°C.min-1 and cooled down at 5°C.min-1.

Electrochemical measurements and HOMO-LUMO calculation were performed in solution. A solution of 0.1 g.L-1 of the investigated polymer in CH_2Cl_2 with 0.1 M tetrabutylammonium hexafluorophosphate (TBAPF6) as electrolyte was prepared. Cyclic voltammetry (CV) measurements were then performed on the solution using silver wire as reference electrode and platinum for the working and counter electrodes. A solution of ferrocene (1 mM in the same solvent) was prepared in the same conditions and the redox potential of Fc/Fc+ vs Ag (EFc/Fc+ Ag) was measured, to be used as a reference for calibration.

Synthesis of 6,6′ Dihydroxy 5,5′ dimethoxy [1,1′ biphenyl] 3,3′ dicarboxaldehyde (Divanillin or DV).
A solution of vanillin in acetone was added to acetate buffer saturated in oxygen with laccase from Trametes Versicolor. In these conditions, the dimer formed precipitates and can be recovered by simple filtration. The filtrate has then simply been reloaded in vanillin and oxygen to start again the synthesis. Yield: 85%
^{1}H-NMR (400.20 MHz, $(CD_3)_2SO$, ppm): d 9.69 (s, 2H); 7.57 (d, J=1.9 Hz, 2H); 7.16 (d, J = 1.9 Hz, 2H); 3.76 (s, 6H).
^{13}C NMR (100.63 MHz, $(CD_3)_2SO$, ppm): 191.2; 150.4; 148.16; 128.2; 127.8; 124.6; 109.2; 56.0.
FT IR (ATR, cm 1): ν= 3220, 1676, 1587, 1413, 1245, 1127, 750.

Synthesis of 6,6′-bis-2-ethylhexyl-5,5′-dimethoxy-[1,1′ biphenyl]-3,3′-dicarboxaldehyde (DVEH).
In a dried and nitrogen flushed 100 mL glassware, divanillin (2 g, 6.62 mmol) was solubilized in 20 mL of previously dried DMSO. Then KOH (0.89 mg, 15.9 mmol) was added to the reaction mixture which was heated at 80°C for 2 hours. Then, 2.2 equivalent of the 2-ethylhexyl bromide were added to the reaction mixture and heated for 12 more hours. The reaction mixture was then poured into 300 mL of water and extracted with 100 mL of diethyl ether, 3 times. The crude product recovered after the diethyl ether evaporation, was purified with flash chromatography in a mixture of cyclohexane/ethyl acetate (95/5).
1H NMR (400.20 MHz, $CDCl_3$, ppm): d 9.89 (s, 2H); 7.46 (dd, J=8.7, 1.9 Hz, 4H); 3.95 (s, 6H); 3.81 (m, 4H), 1.39 1.06 (m, 18H), 0.80 (t, J=7 Hz, 6H), 0.69 (t, J=7.4 Hz, 6H). 13C NMR (100.63 MHz, $CDCl_3$, ppm): 91.1, 153.6, 152.1, 132.0, 131.6, 128.6, 109.7, 75.2, 55.9, 40.4, 30.3, 29.1, 23.5, 22.9, 14.1, 11.0.
FT IR (ATR, cm 1): ν= 2918, 2851, 1697, 1574, 1458, 1386, 1275, 1220, 1127, 1042, 995, 860, 763, 622
HRMS (EI+, m/z) [M]+ calculated (%) for $C_{32}H_{46}O_6Na$: 549.3186, found 549.3163

Synthesis of polyazomethines P1A and P2.
In a 10 mL micro wave dedicated glassware, a stoichiometric amount of p phenylenediamine or 2,7 diaminocarbazole and of the previously synthesized DVEH is put in suspension in 5 mL of toluene. Silica (300 mg) was then added with catalytic amount of PTSA and the reaction heated at 130°C for 4 hours using micro-wave irradiation. The crude polymer was then precipitated in methanol to afford the final polymers unless specified otherwise.

Synthesis of polyazomethine P1B and P1C.
In a 10 mL micro wave dedicated glassware, a stoichiometric amount of p phenylenediamine and of the previously synthesized DVEH is put in suspension in 5 mL of toluene. A catalytic amount of PTSA was then added and the reaction heated at 130°C for 5 minutes using microwave irradiation. The solvent is then removed from the crude mixture to give the crude polymer (P1B). This crude is then dissolved in a minimum amount of methylene chloride, and 100mL of methanol are added. The solution turns cloudy. The solvents are then evaporated using rotary evaporator, to obtain a yellow powder which is rinsed with methanol, to give the final polymer P1C.

Characterization of P1.
^{1}H NMR (400.20 MHz, $CDCl_3$, ppm): d 9.89 (s, 0.07H); 8.42 (s, 2H); 7.66 (s, 1.9H); 7.47 (m, 0.2H); 7.37 (m, 1.7H); 6.98 (m, 0.1H); 6.72 (m, 0.2H); 3.99 (s, 6.8H); 3.79 (m, 4.2H); 1.42 1.02 (m, 21.2H); 0.85-0.77 (m, 6.6H); 0.76-0.68 (m, 6.4H)
^{13}C NMR (100.63 MHz, $CDCl_3$, ppm): d 191.3, 153.6, 152.3, 136.0, 132.2, 131.8, 128.4, 122.0, 112.4, 109.9, 109.6, 90.3, 73.6, 56.1, 32.1, 30.3, 29.8, 29.5, 25.9, 25.9, 22.8, 14.3
FT IR (ATR, cm 1): ν= 2924, 2851, 1697, 1581, 1508, 1464, 1264, 1128, 1025, 800, 725, 615
SEC, ^{1}H NMR and TGA traces are available in Supporting Information.

Characterization of P2.
^{1}H NMR (400.20 MHz, $CDCl_3$, ppm): 9,93 (s, 0,03H), 8.55 (m, 2H); 8.05 (m, 1,83H); 7.74 (s, 1,78H); 7.43 (m, 2,77H); 7.13 (m, 2H); 4.55 (s, 1H); 4.03 (s, 6,36H); 3.81 (m, 3,88H), 2.33 (m, 2,23H); 1.95 (m, 2,54H); 1.43 0.96 (m, 50,13H), 0.79 (m, 19,13H),
^{13}C NMR (100.63 MHz, $CDCl_3$, ppm): d 159.3, 153.7, 152.2, 150.2, 149.6, 143.5, 140.0, 132.4, 131.7, 127.2, 122.3, 120.9, 120.7, 120.4, 112.1, 109.8, 109.4, 104.9, 102.2, 75.3, 72.1, 56.1, 40.6, 39.2, 33.8, 31.9, 30.5, 29.6, 29.5 29.3, 29.3, 27.1, 23.7, 23.2, 22.7, 14.3, 14.2, 11.2.
FT IR (ATR, cm 1): ν= 2924, 2851, 1734, 1581, 1446, 1373, 1264, 1227, 1336, 1049, 970, 872, 788, 653
SEC, ^{1}H NMR and TGA traces are available in Supporting Information.

Computational methods.
All computational details are presented in supporting Information.

5. Acknowledgement.

The authors would like to acknowledge CESAMO (Characterization platform of Université de Bordeaux) for Mass spectrometry. Computational time is provided by Université de Bordeaux. The authors would like to acknowledge Dr. Luca Muccioli, Dr. Frédéric Castet & Dr. Katarzyna Brymora for technical discussion on computational approach.

SUPPORTING INFORMATIONS

Computational details (methods) and all supplementary characterization data (NMR, FTIR, SEC, DSC and cyclic voltamograms).

AUTHOR INFORMATION

Corresponding Author

* Cyril.brochon@enscbp.fr
* Eric.cloutet@enscbp.fr
* cramail@enscbp.fr

Present Address

† Arkema, Centre de production de Feuchy, BP 70029, 62051 Saint-Laurent-Blangy Cedex, France

Author Contributions

# Guillaume Garbay and Lauriane Giraud have contributed equally to this work and must be considered both as "first authors". The manuscript was written through contributions of all authors and they have given approval to the final version of the manuscript.

Funding Sources

This work was funded by Solvay Company, Région Nouvelle Aquitaine and also the French State grant ANR-10-LABX-0042-AMADEus managed by the French National Research Agency under the initiative of excellence IdEx Bordeaux program (reference ANR-10-IDEX-0003-02).

ABBREVIATIONS

DMSO, Dimethyl sulfoxide; DSC, Dynamic scanning calorimetry; HOMO, Highest occupied molecular orbital; LUMO, Lowest unoccupied molecular orbital; NMR, Nuclear Magnetic Resonance

REFERENCES

1. Llevot, A.; Grau, E.; Carlotti; S.; Grelier, S.; Cramail, H. Renewable (semi)aromatic polyesters from symmetrical vanillin-based dimers, *Polym. Chem.*, 2015, **6**, 6058–6066.
2. Kobayashi, S.; Makino, A. Enzymatic Polymer Synthesis: An Opportunity for Greeen Polymer Chemistry, *Chem. Rev.*, 2009, **109**, 5288–5353.
3. Fache, M.; Boutevin, B.; Caillol, S. Epoxy thermosets from model mixtures of the lignin-to-vanillin process, *Green Chem.*, 2016, **18**, 712–725.
4. Llevot, A.; Grau, E.; Carlotti, S.; Grelier, S.; Cramail, H. Selective laccase-catalyzed dimerization of phenolic compounds derived from lignin: Towards original symmetrical bio-based (bis) aromatic monomers, *J. Mol. Catal. B: Enzym.*, 2016, **125**, 34-41.
5. Llevot, A.; Grau, E.; Carlotti, S.; Grelier, S.; Cramail, H. From Lignin-derived Aromatic Compounds to Novel Biobased Polymers, *Macromol. Rapid Commun*., 2016, **37**, 9-28.
6. Gaur, M.; Lohani, J.; Balakrishnan, V. R.; Raghunathan, P.; Eswaran, S. V. Dehydrodivanillin: Multi-dimensional NMR Spectral Studies, Surface Morphology and Electrical Characteristics of Thin Films, Bull. Korean Chem. Soc., 2009, sq30, 2895–2898.
7. Adams, R.; Bullock, J. E.; Wilson, W. C. Contribution to the structure of benzidine, *J. Am. Chem. Soc.*, 1923, **45**, 521–527.
8. Marvel, C. S.; Hill, H. W. Polyazines, *J. Am. Chem. Soc.*, 1950, **72**, 4819–4820.
9. Yang, C. J.; Jenekhe, S. A. Conjugated aromatic poly(azomethines). 1. Characterization of structure, electronic spectra, and processing of thin films from soluble complexes, *Chem. Mater.*, 1991, **3**, 878–887.
10. Yang, C. J.; Jenekhe, S. A. Effect of Structure on refracrive Index of Conjugated Polyimines, *Chem. Mater.*, 1994, **6**, 196–203.
11. Yang, C. J.; Jenekhe, S. A. Conjugated Aromatic Polyimines. 2. Synthesis, Structure, and Properties of New Aromatic Polyazomethines, *Macromolecules*, 1995, **28**, 1180–1196.
12. Garbay, G.; Muccioli, L.; Pavlopoulou, E.; Hanifa, A.; Hadziioannou, G.; Brochon, C.; Cloutet, E. Carbazole-based pi-conjugated polyazomethines: Effects of catenation and comonomer insertion on optoelectronic features, *Polymer (Guildf).*, 2017, **119**, 274–284.
13. Lidström, P.; Tierney, J.; Wathey, B.; Westman, J. Microwave assisted organic synthesis - a review, *Tetrahedron*, 2001, **57**, 9225–9283.
14. Kappe, C. O. Controlled microwave heating in modern organic synthesis, *Angew. Chemie Int. Ed.*, 2004, **43**, 6250–6284.
15. Barik, S.; Skene, W. G. Turning-on the Quenched Fluorescence of Azomethines through Structural Modifications, *European J. Org. Chem.*, 2013, **13**, 2563–2572.
16. Thomas, O.; Inganäs, O.; Andersson, M. R. Synthesis and Properties of a Soluble Conjugated Poly(azomethine) with High Molecular Weight, *Macromolecules*, 1998, **31**, 2676–2678.
17. Wang, C.; Shieh, S.; LeGoff, E.; Kanatzidis, M. G. Synthesis and characterization of a new conjugated aromatic poly(azomethine) derivative based on the 3', 4'-dibutyl-α-terthiophene building block, *Macromolecules*, 1996, **29**, 3147–3156.
18. Barik, S.; Bletzacker, T.; Skene, W. G. π-Conjugated Fluorescent Azomethine Copolymers: Opto-Electronic, Halochromic, and Doping Properties, *Macromolecules*, 2012, **45**, 1165–1173.
19. Barik, S.; Friedland, S.; Skene, W. G. Understanding the reversible anodic behaviour and fluorescence properties of fluorenylazomethines - A structure-property study, *Can. J. Chem.*, 2010, **88**, 945–953.
20. Barik, S.; Skene, W. G. A fluorescent all-fluorene polyazomethine - towards soluble conjugated polymers exhibiting high fluorescence and electrochromic properties, *Polym. Chem.*, 2011, **2**, 1091.
21. Iwan, A.; Palewicz, M.; Chuchmała, A.; Gorecki, L.; Sikora, A.; Mazurek, B.; Pasciak G. Opto(electrical) properties of new aromatic polyazomethines with fluorene moieties in the main chain for polymeric photovoltaic devices, *Synth. Met.*, 2012, **162**, 143–153.
22. Tsai F.-C.; Chang C.; Liu C.; Chen W.; Jenekhe S. A. New thiophene - linked conjugated poly (azomethine)s : Theoretical electronic structure, synthesis, and properties, *Macromolecules*, 2005, **38**, 1958–1966.
23. Lee K.-S.; Won J. C.; Jung J. C. Synthesis and characterization of processable conducting polyazomethines, *Die Makromol. Chemie*, 1989, **190**, 1547–1552.
24. Reinhardt, B. A.; Unroe, M. R. Preparation of aromatic Schiff base polymers with oxydecyl pendants for increased solubility, *Polym. Prepr.*, 1990, 620–621.
25. Kuwabara, J.; Yasuda T.; Choi S. J.; Lu W.; Yamazaki K.; Kagaya, S.; Han, L.; and Kanbara, T. Direct arylation polycondensation: A promising method for the synthesis of highly pure, high-molecular-weight conjugated polymers needed for improving the performance of organic photovoltaics, *Adv. Funct. Mater.*, 2014, **24**, 3226–3233.
26. Nayak, S. N.; Bhasin, C. P.; Nayak, M. G. A review on microwave-assisted transesterification processes using various catalytic and non-catalytic systems, *Renew. Energy*, 2019, **143**, 1366–1387.
27. Walba, H., K.; Branch, G. E. K. The Absorption Spectra of

Some N-Substituted p-Aminotriphenylmethyl Ions. *J. Am. Chem. Soc.*, 1951, **1083**, 3341–3348.
28. Boudreault, P.-L. T.; Najari, A.; Leclerc, M. Processable Low-Bandgap Polymers for Photovoltaic Applications. *Chem. Mater.*, 2011, **23**, 456–469.
29. Torras, J.; Casanovas, J.; Alemán, C. Reviewing Extrapolation Procedures of the Electronic Properties on the π-Conjugated Polymer Limit. *J. Phys. Chem. A*, 2012, **116**, 7571–7583.
30. Gierschner, J.; Cornil, J.; Egelhaaf, H. -J. Optical Bandgaps of π-Conjugated Organic Materials at the Polymer Limit: Experiment and Theory. *Adv. Mater.*, 2007, **19**, 173–191.
31. Wykes, M.; Milián-Medina, B.; Gierschner, J. Computational engineering of low bandgap copolymers. *Front. Chem.*, 2013, **1**, 35.

For Table of Contents Only

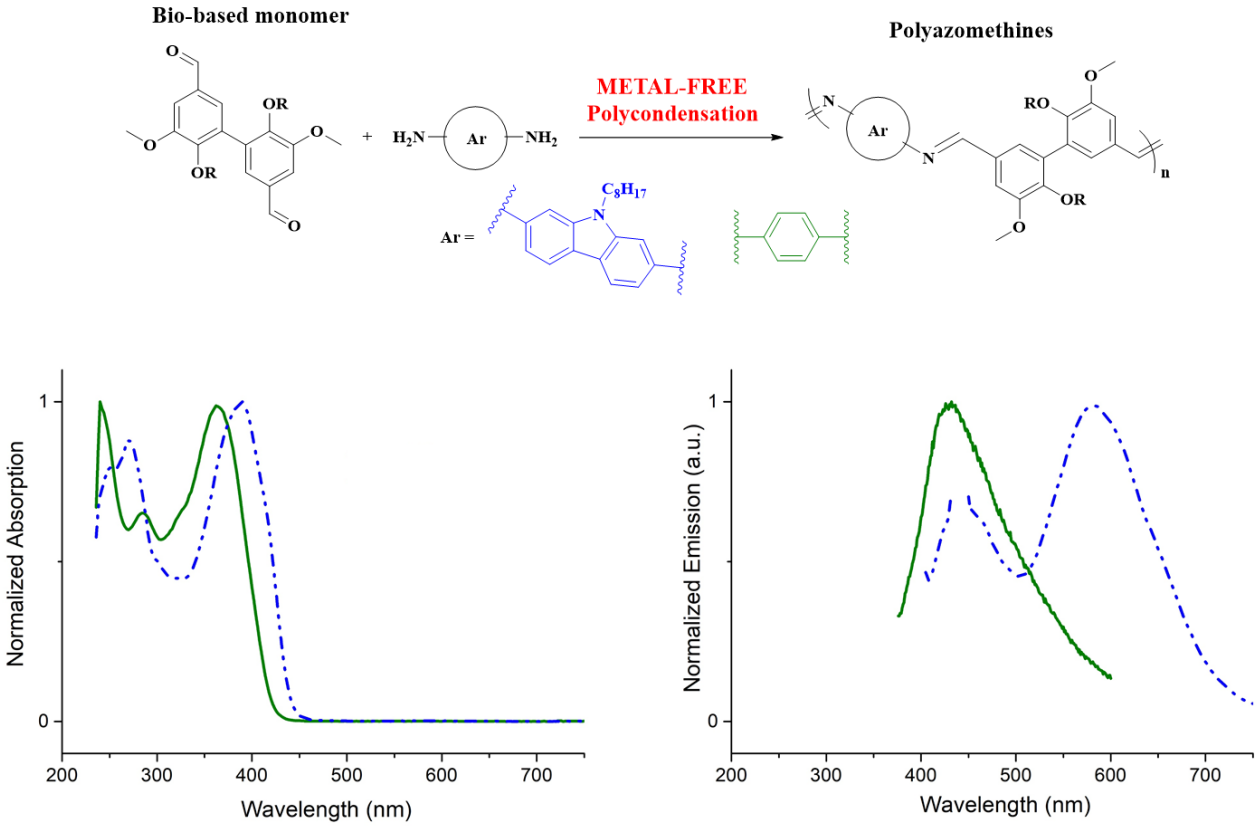

Supporting Information

Divanillin-based polyazomethines: toward bio-based and metal-free π-conjugated polymers

Guillaume Garbay, [†#a] Lauriane Giraud, [#a] Sai Manoj Gali, [a] Georges Hadziioannou, [a] Etienne Grau, [a] Stéphane Grelier, [a] Eric Cloutet, [a] * Henri Cramail, [a] * Cyril Brochon [a] *

[a] Laboratoire de Chimie des Polymères Organiques (LCPO UMR 5629), CNRS-Université de Bordeaux-Bordeaux INP, 16 Avenue Pey-Berland, Pessac, 33607 Cedex, France

† current address : Arkema, Centre de production de Feuchy, BP 70029, 62051 Saint-Laurent-Blangy Cedex, France

Table of contents

Computational Details

1. Electronic and optical properties of monomers

Relaxed potential energy surface scans were first performed on monomer units of **DV-Cbz** and **DV-Ph** to sample the possible stable conformations with respect to the torsional angles around single bonds. Calculations were performed at PBE0/6-31(d,p) level of theory with chloroform as implicit solvent using CPCM implicit solvation model. Three dihedral angles were considered for each derivative, θ_1, θ_2 and θ_3 as shown in **Figure S15**. Corresponding energy scans are presented in **Figure S16**.

The relative energies (ΔE in kcal/mol) of the various stable conformers obtained from the Potential Energy Surface (PES) scans are collected in **Table S1**.

In a second step, **DV-Ph** and **DV-Cbz** derivatives were fully optimized by starting from the lowest-energy conformer obtained from the PES scans. Optimizations were carried out at the DFT level using the 6-31(d,p) basis set with various exchange-correlation functionals (XCFs) and chloroform as implicit solvent. Frequency calculations were then performed to ensure proper optimization of the geometries. **Table S2** reports the HOMO and LUMO energies (in eV), as well as the electronic band gap ($E_G = E_{LUMO} - E_{HOMO}$) of both derivatives, for a selection of exchange-correlation functionals (XCFs). Irrespective of the DFT functional employed, $E_{G-\mathbf{DV\text{-}Cbz}} < E_{G-\mathbf{DV\text{-}Ph}}$.

Furthermore, vertical transition energies (E_{Vert}) were computed at the time-dependent DFT (TD-DFT) level using the same XCFs and basis set as those employed in geometry optimizations. Consistently with the electronic band gap, results collected in **Table S2** also show that $E_{Vert-\mathbf{DV\text{-}Cbz}} < E_{Vert-\mathbf{DV\text{-}Ph}}$, irrespective of the choice of XCF selected.

2. Electronic and optical properties of increasing-size oligomers

Similar DFT and TD-DFT calculations were then carried out on increasing-size oligomers of both derivatives, using the B3LYP and CAM-B3LYP functionals. B3LYP was selected since it provides good estimate of the HOMO and LUMO energy levels compared to those deduced experimentally from cyclic voltammetry measurements, although such comparisons are highly approximate. CAM-B3LYP was selected because it is known to improve the description of low-lying charge-transfer excited states in push-pull dyes [S1]. Electronic band gaps (E_G) and vertical transition energies (E_{Vert}) as a function of chain length of the oligomers are gathered in **Table S3**. Irrespective of the increase in chain length, $E_{G-\mathbf{DV\text{-}Cbz}} < E_{G-\mathbf{DV\text{-}Ph}}$.

3. Electronic and optical gaps at polymer limit

Finally, the size-converged electronic and optical gaps were evaluated using a fitting procedure based on the Khun's model, which is based on linear coupling of double bonds (harmonic oscillators) that contribute to electronic transitions.[S2, S3] In this procedure, the electronic gap or vertical transition energies reported in **Table S3** are first plotted against 1/N, where N is the number of double bonds along the shortest conjugated pathway connecting the terminal carbon of the oligomers. Then, a linear regression can be obtained based on Khun's equation (Equation 1) to extract energy gaps at polymer limit:

$$E_g = E_0\sqrt{1 + D_k cos\left(\frac{\pi}{N+1}\right)} \quad (1)$$

In the above equation, E_0 and D_k are the fitting parameters. E_0 corresponds to the energy gap when N = 1 and D_k is a force constant that represents the strength of coupling between single and double bonds in a given oligomer, entailing that D_k is implicitly linked to the efficiency of the π-conjugation between consecutive monomeric units (higher the value of D_k, higher the delocalization of π electrons).[S4]

The evolution of the electronic and optical gaps as a function of 1/*N*, calculated at the B3LYP/6-31G(d) and CAM-B3LYP/6-31G(d) levels, are shown in **Figure S17**. The size-converged electronic and optical gaps, as well as the optimized E_0 and D_k parameters, are reported in **Table S4**. The two levels of calculation predict that the **DV-Cbz** derivative shows lower electronic and optical gaps at polymer limit than the **DV-Ph** derivative. This relative ordering both originates from a lower value of the band gap of the **DV-Cbz** monomer (see section 1), and from a more efficient π-conjugation between consecutive units, as indicated by the larger D_k values.

References

[S1] Jacquemin, D.; Perpète, E. A.; Scuseria, G. E.; Ciofini, I. ; Adamo, C. TD-DFT Performance for the Visible Absorption Spectra of Organic Dyes: Conventional versus Long-Range Hybrids, *J. Chem. Theory Comput.*, **2008**, *4*, 1.

[S2] Gierschner, J.; Cornil, J.; Egelhaaf, H.-J. Optical Bandgaps of π‐Conjugated Organic Materials at the Polymer Limit: Experiment and Theory, *Advanced Materials*, **2007**, *19*, 173.

[S3] Torras, J.; Casanovas, J.; Alemn, C. Reviewing Extrapolation Procedures of the Electronic Properties on the π-Conjugated Polymer Limit, *The Journal of Physical Chemistry A*, **2012**, *116*, 7571.

[S4] Wykes, M.; Milin-Medina, B.; Gierschner, J. Computational engineering of low bandgap copolymers, *Frontiers in Chemistry*, **2013**, *1*, 35.

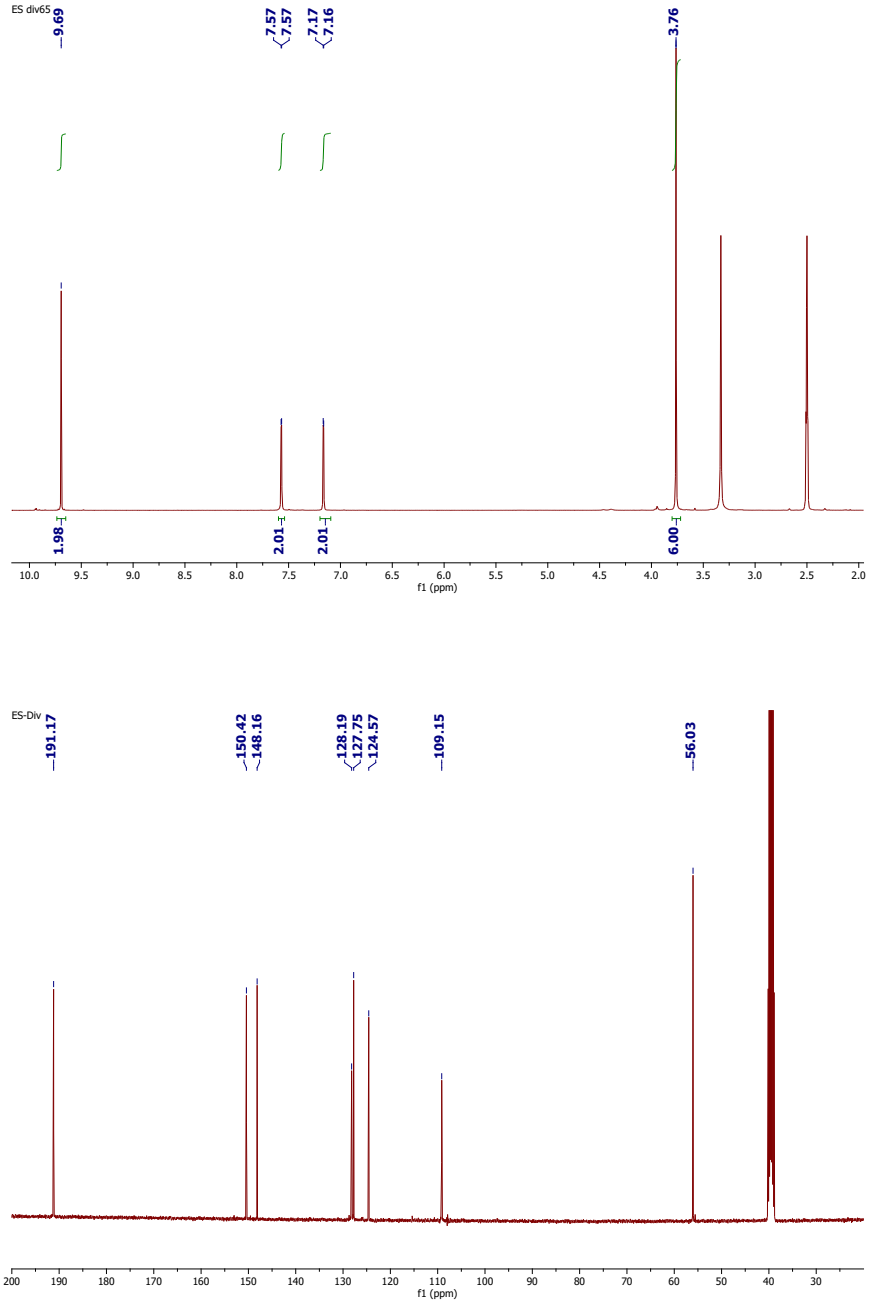

Figure S1. ^{1}H-NMR (top) and ^{13}C-NMR (bottom) spectra of **DV** (400.20 MHz and 100.63 MHz respectively, in $(CD_3)_2SO$)

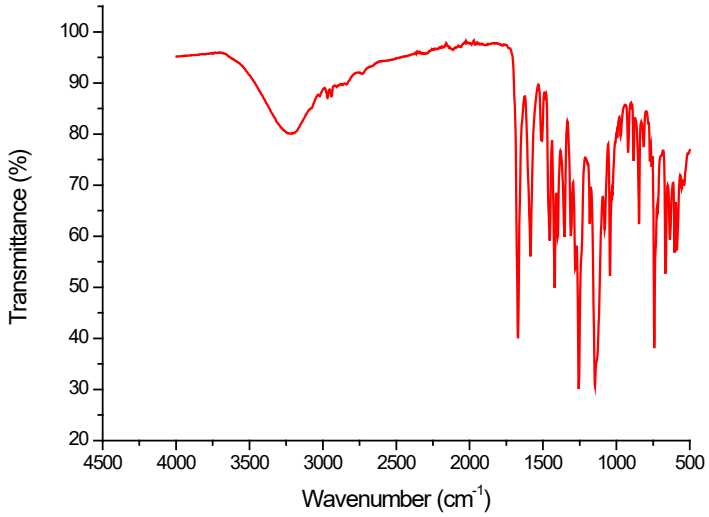

Figure S2. ATR-FTIR spectrum of **DV**

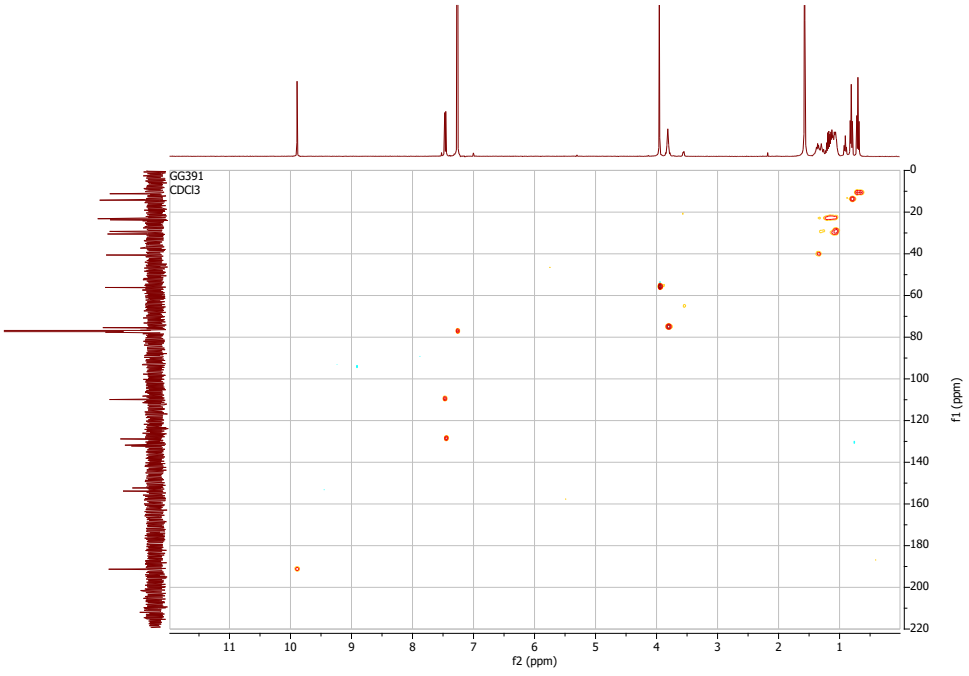

Figure S3. ^{1}H-^{13}C HSQC NMR spectrum of **DVEH** (400.20 MHz and 100.63 MHz respectively, in $CDCl_3$)

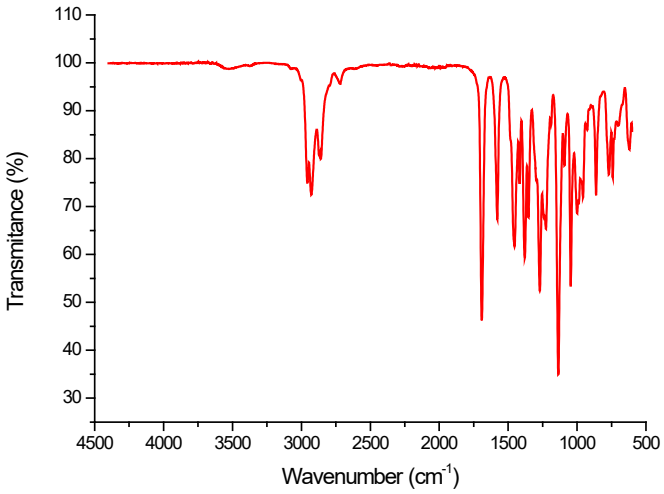

Figure S4. ATR-FTIR spectrum of **DVEH**

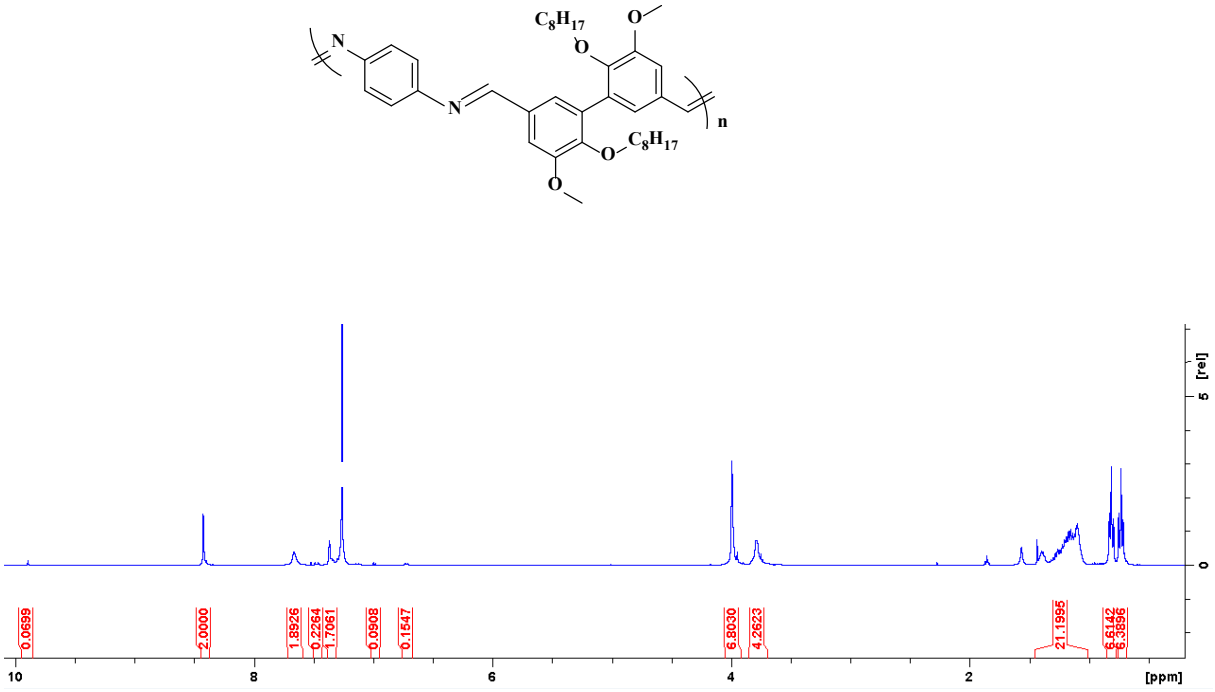

Figure S5. ^{1}H-NMR spectrum of **P1A** (400.20 MHz, in $CDCl_3$)

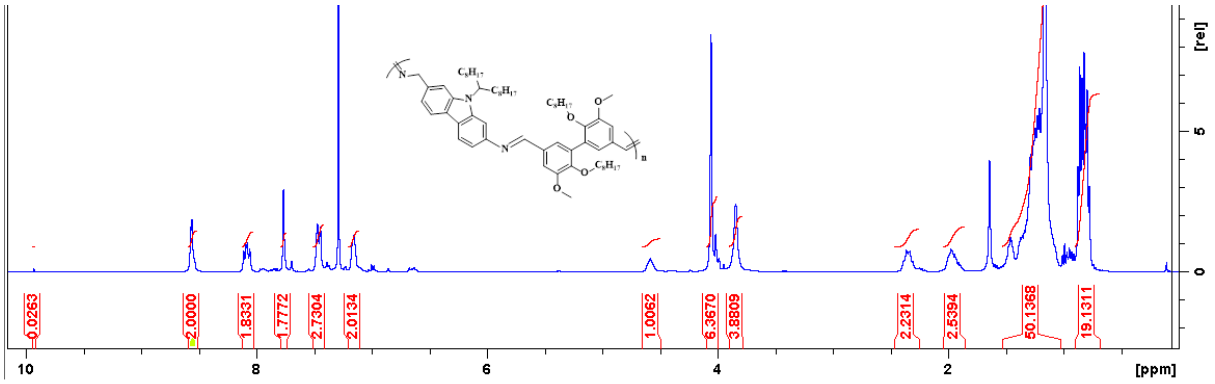

Figure S6. ^{1}H-NMR spectrum of **P2** (400.20 MHz, in $CDCl_3$)

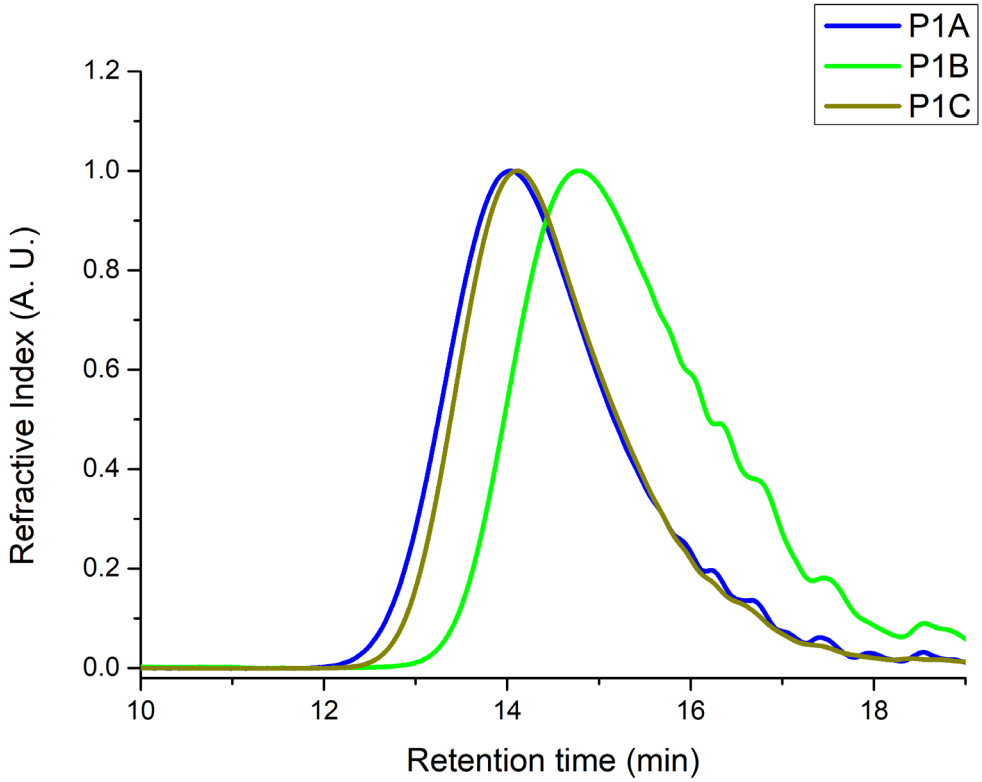

Figure S7. SEC traces of **P1A**, **P1B** and **P1C** (in THF, polystyrene standard)

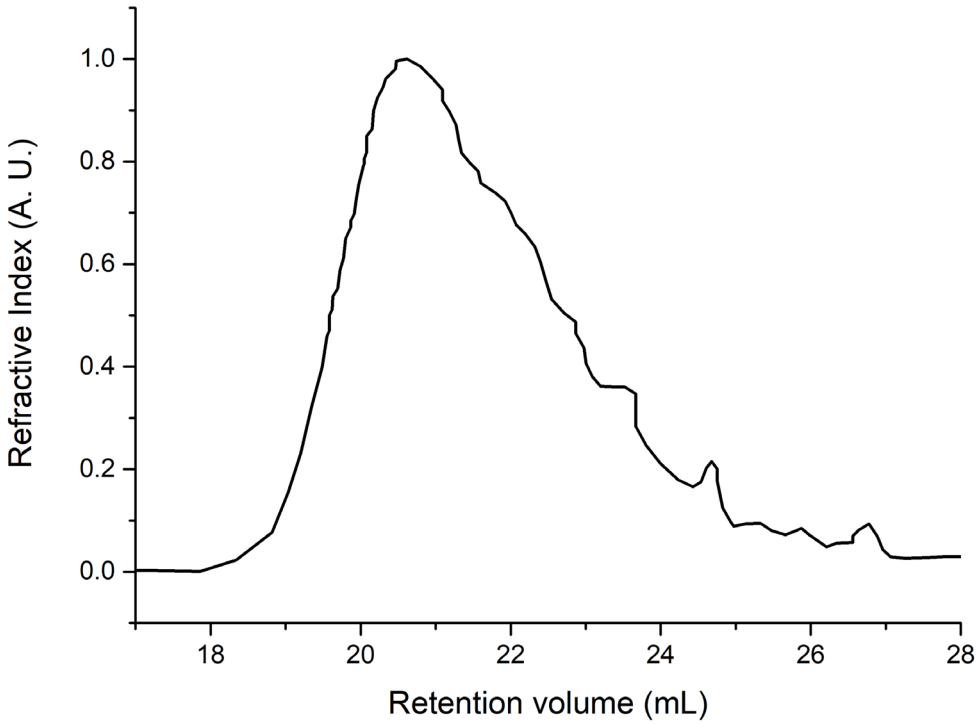

Figure S8. SEC trace of **P2** (in THF, polystyrene standard)

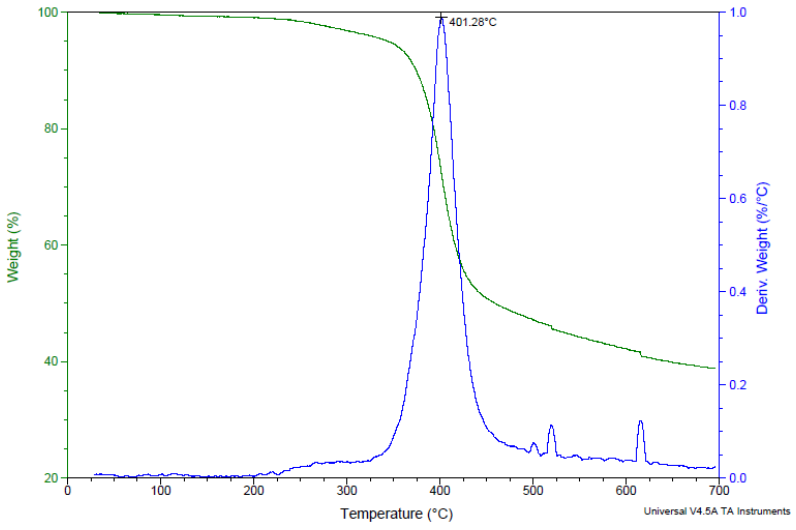

Figure S9. TGA trace of **P1A**

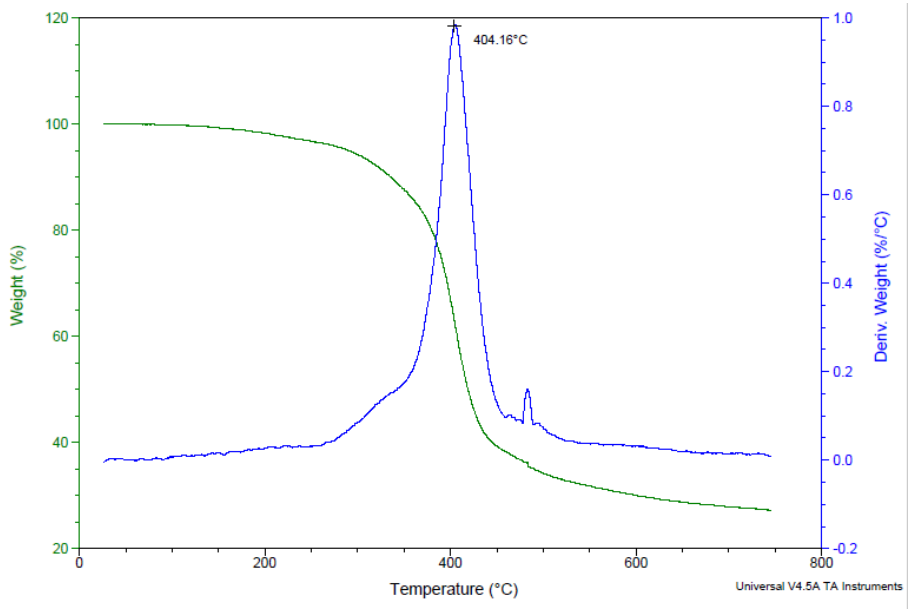

Figure S10. TGA trace of **P2**

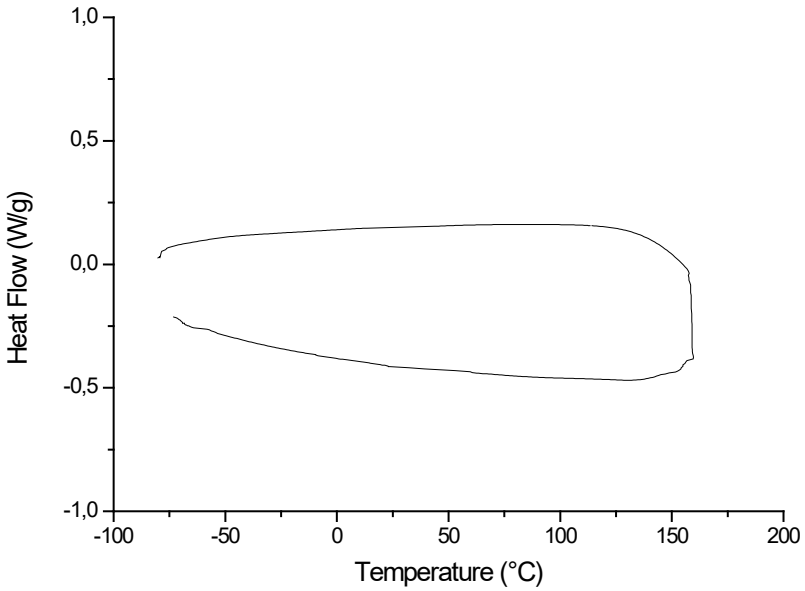

Figure S11. DSC trace of **P1A**

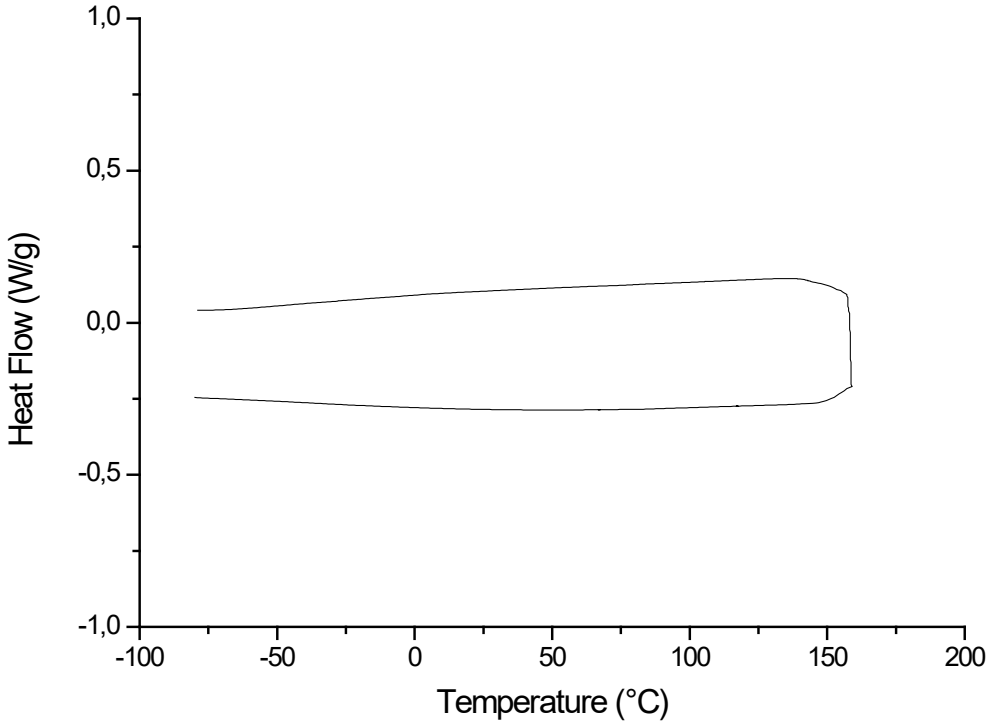

Figure S12. DSC trace of **P2**

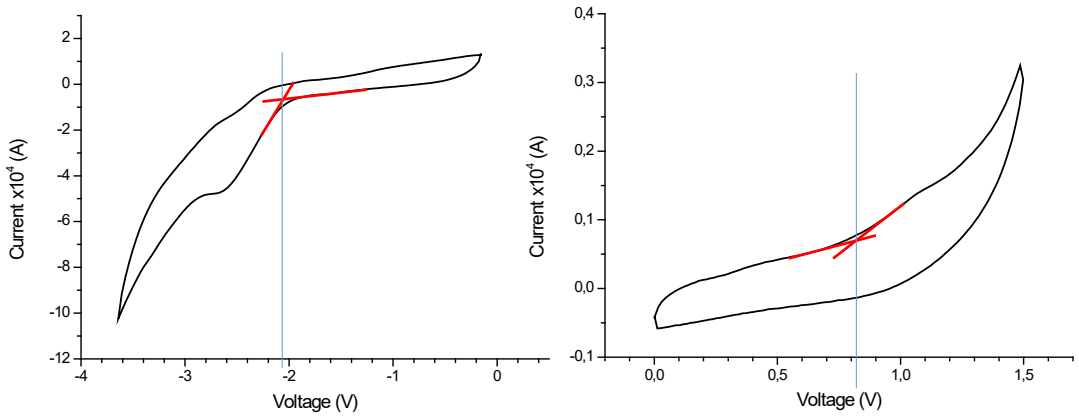

Figure S13. Cyclic voltammograms (left-reduction, right-oxidation) of **P1A** in CH_2Cl_2 solution

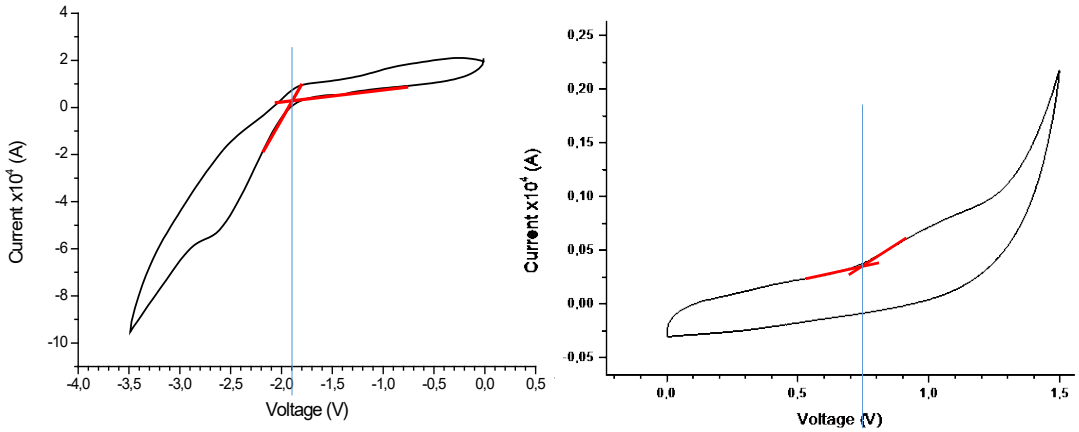

Figure S14. Cyclic voltammograms (left-reduction, right-oxidation) of **P2** in CH_2Cl_2 solution

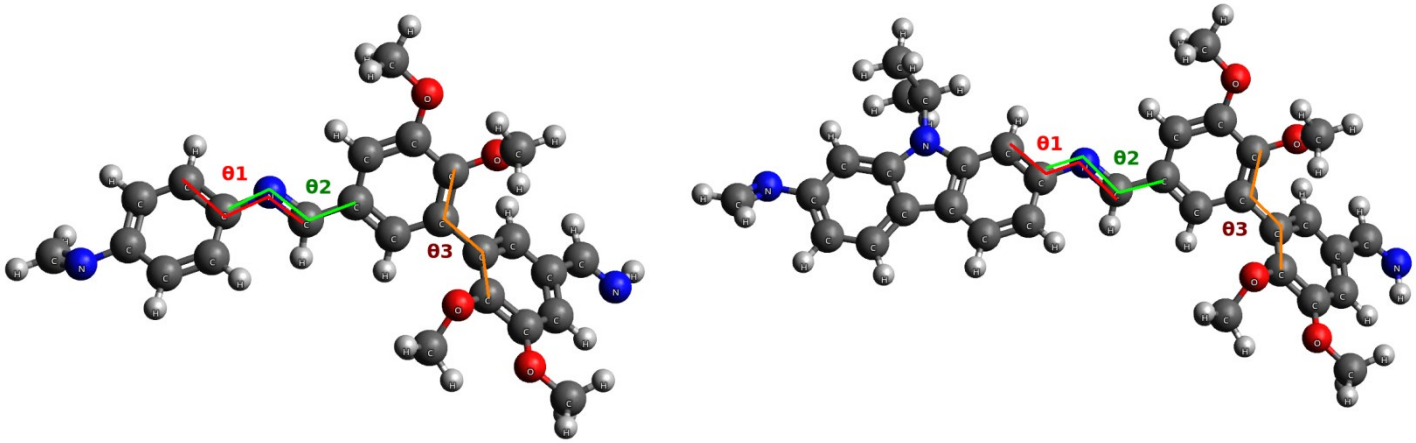

Figure S15. Dihedrals considered for the relaxed potential energy surface scans in monomers of (left) **DV-Ph** and (right) **DV-Cbz** derivatives

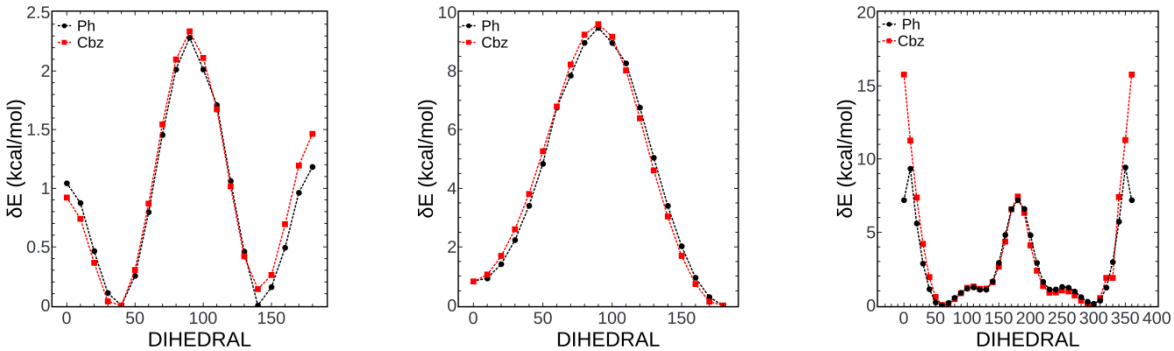

[a] Dihedral: θ_1 [b] Dihedral: θ_2 [c] Dihedral: θ_3

Figure S16. Relaxed potential energy surface scans with respect to dihedrals θ_1, $\theta_2$and θ_3 for monomers of **DV-Ph** (Ph: Black - Circles) and **DV-Cbz** (Cbz: Red - Squares)

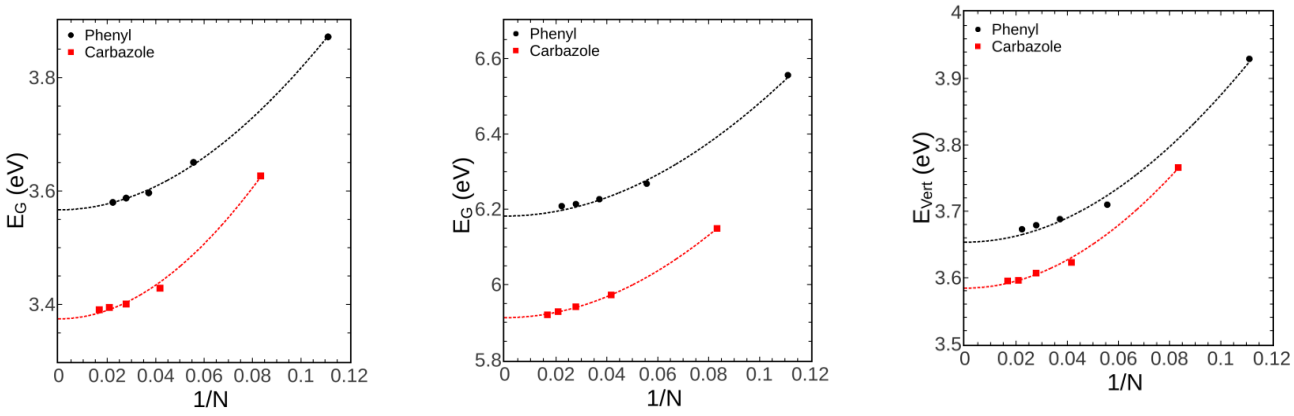

[a] B3LYP: E_G [b] CAM-B3LYP: E_G [c] CAM-B3LYP: E_{Vert}

Figure S17. Evolution with chain length of the electronic gap of increasing-size **DV-Cbz** (red) and **DV-Ph** (black) oligomers, as calculated at the (a, left) B3LYP/6-31G(d) and (b, centre) CAM-B3LYP/6-31G(c) levels. The right panel reports the evolution of the vertical transition energy (E_{Vert}) calculated at the CAM-B3LYP/6-31G (c) level. Dotted lines are Khun fits

Derivative / Dihedral	θ_1	θ_2	θ_3	ΔE (kcal/mol)
DV-Ph	40.0	177.48	126.39	1.020
	140.0	177.53	126.31	1.149
	39.55	0.0	126.51	1.864
	39.89	180.0	126.84	1.036
	40.08	**176.98**	**60.0**	**0.0**
	39.73	176.96	120.0	1.072
DV-Cbz	40.0	177.61	126.27	0.937
	140.0	176.77	125.32	0.937
	40.81	0.0	126.67	1.081
	41.11	180.0	125.18	1.895
	39.30	**177.69**	**60.0**	**0.0**
	40.18	176.59	120.0	1.098

Table S1. Stable conformers obtained from the PES scans for θ_1, θ_2 and θ_3 and relative energies (ΔE in kcal/mol)

Functional	**DV-Ph**					**DV-Cbz**					$\Delta E_{(Phnl-Crbz)}$	
	HOMO	LUMO	E_G	λ_{max}	E_{Vert}	HOMO	LUMO	E_G	λ_{max}	E_{Vert}	ΔE_G	ΔE_{Vert}
PBE0	-5.952	-1.643	4.309	352	3.516	-5.631	-1.622	4.009	376	3.294	0.300	0.222
B3LYP	-5.625	-1.753	3.872	394	3.375	-5.329	-1.702	3.627	394	3.104	0.245	0.235
CAM-B3LYP	-7.037	-0.480	6.556	315	3.930	-6.632	-0.483	6.149	329	3.766	0.407	0.164
wB97XD	-7.599	-0.051	7.548	313	3.951	-7.220	-0.065	7.155	323	3.834	0.393	0.117
M06HF	-8.797	-0.446	8.350	301	4.107	-8.286	-0.353	7.933	304	4.071	0.417	0.036
M062X	-6.964	-0.827	6.137	319	3.886	-6.597	-0.861	5.736	333	3.716	0.401	0.170

Table S2. Electronic (E_G) and optical (E_{Vert}) gaps (in eV), as well as maximum absorption wavelengths (in nm) of **DV-Cbz** and **DV-Ph** derivatives calculated at the TD-DFT level using various XCFs with the 6-31(d,p) basis set. $\Delta E_{(Phnl-Crbz)}$ corresponds to differences between the electronic/optical gaps of the two derivatives

Functional	Unit	DV-Cbz			DV-Cbz			$\Delta E_{G(Phnl-Crbz)}$
		HOMO	LUMO	E_G	HOMO	LUMO	E_G	ΔE_G
[a] B3LYP	Monomer	-5.625	-1.753	3.872	-5.329	-1.702	3.627	0.245
	Dimer	-5.516	-1.894	3.621	-5.224	-1.795	3.429	0.192
	Trimer	-5.507	-1.909	3.597	-5.214	-1.803	3.411	0.186
	Tetramer	-5.500	-1.911	3.588	-5.203	-1.808	3.395	0.190

Functional	Unit	**DV-Ph**					**DV-Cbz**					$\Delta E_{G(Phnl-Crbz)}$	
		HOMO	LUMO	E_G	λ_{max}	E_{Vert}	HOMO	LUMO	E_G	λ_{max}	E_{Vert}	ΔE_G	ΔE_{Vert}
[b] CAM-B3LYP	Monomer	-7.037	-0.480	6.556	315	3.930	-6.632	-0.483	6.149	329	3.766	0.407	0.164
	Dimer	-6.879	-0.623	6.248	334	3.712	-6.553	-0.580	5.973	342	3.623	0.275	0.089
	Trimer	-6.862	-0.634	6.227	336	3.688	-6.535	-0.594	5.941	343	3.607	0.286	0.081
	Tetramer	-6.857	-0.642	6.210	337	3.679	-6.529	-0.601	5.928	344	3.596	0.285	0.083

Table S3. Electronic (E_G) and optical (E_{Vert}) gaps (in eV), as well as maximum absorption wavelengths (in nm) of increasing-size **DV-Cbz** and **DV-Ph** derivatives, as calculated at the [a] B3LYP/6-31G(d) and [b] CAM-B3LYP/6-31G(d) levels. $\Delta E_{(Phnl-Crbz)}$ corresponds to differences between the electronic/optical gaps of the two derivatives

Derivative / Functional	**DV-Cbz**			**DV-Ph**		
	E_g	E_0	D_k	E_g	E_0	D_k
B3LYP	3.390	7.923	0.818	3.580	7.105	0.715
CAM-B3LYP	5.920	10.90	0.748	6.210	10.76	0.668

Table S4. Electronic band gap and vertical transition energies at the polymer limit (E_g in eV), and optimized E_0 and D_k parameters (in eV, extracted from Equation 1) for **DV-Cbz** and **DV-Ph** derivatives.